

Time Series Analysis of Nonlinear Head Dynamics Using Synthetic Data Generated with a Variably Saturated Model

Vonk, Martin A.; Collenteur, Raoul A.; Panday, Sorab; Schaars, Frans; Bakker, Mark

DOI

[10.1111/gwat.13403](https://doi.org/10.1111/gwat.13403)

Publication date

2024

Document Version

Final published version

Published in

Groundwater

Citation (APA)

Vonk, M. A., Collenteur, R. A., Panday, S., Schaars, F., & Bakker, M. (2024). Time Series Analysis of Nonlinear Head Dynamics Using Synthetic Data Generated with a Variably Saturated Model. *Groundwater*, 62(5), 748-760. <https://doi.org/10.1111/gwat.13403>

Important note

To cite this publication, please use the final published version (if applicable). Please check the document version above.






Copyright

Other than for strictly personal use, it is not permitted to download, forward or distribute the text or part of it, without the consent of the author(s) and/or copyright holder(s), unless the work is under an open content license such as Creative Commons.

Takedown policy

Please contact us and provide details if you believe this document breaches copyrights. We will remove access to the work immediately and investigate your claim.

Time Series Analysis of Nonlinear Head Dynamics Using Synthetic Data Generated with a Variably Saturated Model

by Martin A. Vonk^{1,2,3} , Raoul A. Collenteur⁴ , Sorab Panday⁵ , Frans Schaars² , and Mark Bakker¹ 

Abstract

The performance of time series models is assessed using synthetic head series simulated with a numerical model that solves Richards' equation for variably saturated flow. Heads were simulated in a homogeneous unconfined aquifer between two parallel canals; measured daily precipitation and potential evaporation are specified at the land surface and root water uptake is simulated. The head response to a precipitation event is nonlinear and depends on the saturation degree and rainfall before and after the precipitation event while evaporation reduction occurs during summers. Synthetic series were generated for 27 years and three different soil types; the unsaturated zone thickness varies between 0 and >5 m. The synthetic head series were simulated with a linear and nonlinear time series model. Performance of a linear time series model with four parameters, using a scaled Gamma response, gave R^2 values ranging from 0.67 to 0.96. The nonlinear time series model with five parameters simulates recharge using a root zone reservoir after which the head response to recharge is simulated with a scaled Gamma response function. The nonlinear time series model was able to simulate all synthetic head series very well with R^2 values above 0.9 for almost all models. The head response of the nonlinear model to a single precipitation event compares well to the response of the variably saturated groundwater model. The provided scripts may be used to simulate synthetic head series for other climates or for systems with additional complexity to assess the performance of other data-driven models.

Introduction

Head fluctuations can be simulated with a variety of groundwater models. White box groundwater models describe the physical processes using deterministic equations. These kinds of models often need detailed

knowledge of both the subsurface and the boundary conditions. As a result, they need extensive parameterization and are time-consuming to develop. In contrast to white box models, black box models are entirely data-driven. Black box models try to determine a relation between input and output series purely from the data, without any physical understanding of the system (Bakker and Schaars 2019). In the current age of big data, these black box models are becoming increasingly popular. Siegel and Hinchey (2019) argued, however, that black box models “neglect centuries of scientific understanding of physical processes to empirically look for relationships among data that underlie all natural phenomena.”

A compromise between white and black is a gray box model, also referred to as a semi-physical model, a lumped parameter model, or a reduced order model, which applies algorithms that have some physical basis. In groundwater hydrology, time series models using predefined response functions (e.g., von Asmuth et al. 2002) are a popular gray box method to simulate head fluctuations. The response functions that are used in this method have a semiphysical basis and only a few parameters, which make these models relatively simple and fast. The method may be applied to simulate groundwater dynamics caused by a variety of stresses (also called forcings or drivers), such as areal recharge, pumping, or

¹Department of Water Management, Faculty of Civil Engineering and Geosciences, Delft University of Technology, Delft, South Holland, The Netherlands

²Artesia B.V., Schoonhoven, South Holland, The Netherlands

³Corresponding author: Department of Water Management, Faculty of Civil Engineering and Geosciences, Delft University of Technology, Delft, South Holland, The Netherlands; m.a.vonk@tudelft.nl

⁴Department Water Resources and Drinking Water, Eawag, Dübendorf, Zürich, Switzerland

⁵GSI Environmental Inc., Herndon, Virginia, United States

Article impact statement: Nonlinear time series models with a few parameters can simulate synthetic head series generated with a variably saturated numerical model.

Received October 2023, accepted March 2024.

© 2024 The Authors. *Groundwater* published by Wiley Periodicals LLC on behalf of National Ground Water Association.

This is an open access article under the terms of the [Creative Commons Attribution-NonCommercial](https://creativecommons.org/licenses/by-nc/4.0/) License, which permits use, distribution and reproduction in any medium, provided the original work is properly cited and is not used for commercial purposes.

doi: 10.1111/gwat.13403

surface water fluctuations (von Asmuth et al. 2008). Areal recharge is often approximated as a linear combination of precipitation and potential evaporation, referred to as a linear recharge model. Simple linear recharge models give remarkably good results, especially in temperate oceanic climates with relatively shallow water tables (e.g., von Asmuth et al. 2002; Zaadnoordijk et al. 2019).

Linear recharge models are a simplification of the highly nonlinear flow through the unsaturated zone where the hydraulic conductivity depends on the soil water content (e.g., Feddes et al. 1988). The lack of incorporation of these nonlinear processes may result in poor fits and predictions, especially for groundwater systems with (relatively) thick unsaturated zones (Hunt et al. 2008; Zaadnoordijk et al. 2019) and in warmer climates where actual evaporation cannot be approximated as a linear function of potential evaporation (Peterson and Western 2014).

Nonlinear recharge models were developed to convert the measured precipitation and potential evaporation into recharge using a nonlinear approach. Several studies have investigated the use of nonlinear recharge models. Berendrecht et al. (2006) introduced nonlinearity by modeling the degree of water saturation of the root zone. Peterson and Western (2014) added a flexible vertically integrated soil moisture module to account for nonlinear processes. More recently, Collenteur et al. (2021) proposed a nonlinear recharge model based on a soil–water balance approach. Although the results of these studies are promising, nonlinear time series models need further development and testing (Peterson and Western 2014; Collenteur et al. 2021).

Linear and nonlinear time series models are, obviously, an approximation of the groundwater system and their usefulness in simulating dynamics in real world aquifers needs to be assessed. Berendrecht et al. (2006), Peterson and Western (2014), and Collenteur et al. (2021) all assessed the performance by applying their model to measurements. Another approach to assess the performance is to use synthetic head series that are generated with a white box, physics-based groundwater model. The main advantage of such an approach is that the “truth” is known (the groundwater model), which facilitates the comparison of results in a controlled setting. A disadvantage is that it is a challenge to make a synthetic model that incorporates all the processes and heterogeneity of a real system, especially in the unsaturated zone and at the land surface. Random or correlated errors can be added to input series and/or generated synthetic head series, which allows for the testing of the effect of the signal-to-noise ratio. Several studies demonstrated good performance of linear time series models using synthetic head series obtained from analytic or numerical groundwater models (Bakker et al. 2007, 2008; Klop 2019); all these studies used synthetic series from a model that only simulated flow in the saturated zone using weather data for a temperate oceanic climate. Shapoori et al. (2015) also investigated the effect of the unsaturated zone. In this study, synthetic head series were generated to assess

whether the contribution of pumping could be estimated in a system with both pumping and recharge. This was done by simulating flow in a single-layer MODFLOW model using the Unsaturated Zone Flow (UZF) package (Niswonger et al. 2006) to simulate recharge for the temperate oceanic climate in south-eastern Australia. They used the nonlinear time series model of Peterson and Western (2014) and identified a range of head variations for which they were able to extract the pumping signal from the synthetic series. Romano et al. (2011) simulated soil moisture and fluxes with a bucket model and obtained good results when compared with a one-dimensional unsaturated zone model solving Richards’ equation.

The objective of this article is to assess the performance of nonlinear time series models to simulate groundwater dynamics using synthetic head data generated with a physics-based numerical model that simulates two-dimensional variably saturated flow by solving Richards’ equation (Richards 1931). The synthetic head data is generated using MODFLOW USG-Transport (Panday 2023); USG stands for UnStructured Grid, but a structured grid is used in this article. Measured daily precipitation and potential evaporation are used for a temperate oceanic climate. The performance of the nonlinear time series model of Collenteur et al. (2021) in simulating the synthetic head series is assessed using the Pastas time series model (Collenteur et al. 2019). No errors or noise are added to either the generated synthetic heads or the precipitation and evaporation series, so any mismatch is solely caused by limitations of the nonlinear time series model (i.e., model structural error). Several soil types and thicknesses of the unsaturated zone are considered for flow between two parallel canals in a homogeneous aquifer. Inhomogeneous aquifers as well as tropical, arid, or continental climates are interesting but are not considered here to keep the scope of the article manageable.

This article is structured as follows. First, the generation of synthetic head series is discussed, which includes a description of the system, the selected soil types and equations for variably saturated flow and evaporation via root uptake, the numerical model used to generate the synthetic heads, the measured meteorological series, and finally an example synthetic head series. Second, the nonlinear behavior of the head response, as simulated with the variably saturated model, is discussed in detail. Third, the nonlinear time series model and the performance metrics are described. Finally, the performance of the nonlinear time series model to simulate the synthetic head series is assessed, followed by a discussion and conclusions.

Generation of the Synthetic Head Series

A groundwater model for variably saturated flow is used to generate synthetic head series and investigate the impact of the unsaturated zone on the groundwater dynamics. These synthetic head series are used later on in the article to assess the performance of the time series models. Synthetic series are generated for a system that consists of an aquifer between

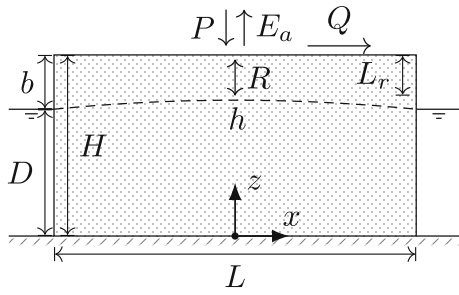


Figure 1. System of a homogeneous aquifer between two parallel canals.

two parallel, fully penetrating canals, as depicted in Figure 1. Flow is two-dimensional in the vertical plane and is governed by Richards' equation (Richards 1931). The canals are a distance L (L) apart with the origin of the coordinate system chosen at the bottom of the aquifer, halfway between the canals. The bottom of the aquifer is a no-flow boundary. The head along the left ($x = -\frac{L}{2}$) and right ($x = \frac{L}{2}$) boundaries is specified as hydrostatic where the canal stage is fixed to $z = D$ (L) on both sides. The difference between the ground surface H and the canal stage D is called the freeboard b , which is equal to the unsaturated zone thickness at the left and right boundaries. At other locations in the aquifer, the thickness of the unsaturated zone varies in space and time. The flux along the top boundary ($z = H$) is specified as the precipitation flux P (L/T). The actual evaporation E_a (L/T) is computed as transpiration from the root zone, with a rooting depth L_r , for a specified potential evaporation flux E_p (L/T). The flux R (L/T) represents groundwater recharge when it is positive (downward) and capillary rise when it is negative (upward). When the head h (L) reaches the ground surface H , surface runoff Q (L/T) is generated using MODFLOW's drain package (Harbaugh 2006).

Soil Types

Three different soil types are considered in this study: sand, sandy loam, and silt loam (as defined by Carsel and Parrish 1988). These soils are chosen to cover a range of hydraulic soil properties. The water content θ of the soils, defined as the volume of water divided by the total volume, is described by the van Genuchten equation (van Genuchten 1980)

$$\theta(\psi) = \begin{cases} \theta_r + \frac{\theta_s - \theta_r}{(1 + |\alpha|\psi - \psi_b|^\beta)^{1-1/\beta}} & \text{for } \psi \leq 0 \\ \theta_s & \text{for } \psi > 0 \end{cases}, \quad (1)$$

where θ_r (–) is the residual water content, θ_s (–) is the saturated water content, α (L⁻¹) and β (–) are the van Genuchten parameters, ψ (L) is the pressure head, and ψ_b (L) is the air entry pressure head. The pressure head is computed from the hydraulic head h as $\psi = h - z$, where z is the elevation. The hydraulic conductivity K (L/T) in the unsaturated zone is described by the Brooks-Corey

equation (Brooks and Corey 1964)

$$K(\theta) = K_r(\theta)K_s = \left(\frac{\theta - \theta_r}{\theta_s - \theta_r}\right)^\varepsilon K_s, \quad (2)$$

where K_r (–) is the relative permeability, K_s (L/T) is the saturated conductivity, and ε (–) is the Brooks–Corey exponent.

The van Genuchten soil model parameters for the three soil types are obtained from van Genuchten et al. (1991, tab. 4). The Brooks–Corey exponent ε is obtained by fitting the Brooks–Corey relative permeability curve to the van Genuchten relative permeability curve (van Genuchten 1980). The fitting routine uses least squares for the values of $\psi \in \{10^{-4}, 10^{-3}, \dots, 10^6 \text{ cm}\}$. The soil water retention curves and hydraulic conductivity functions for the three soil types can be found in Supporting Information S1. The specific storage S_s is chosen at a value of 10^{-6} m^{-1} for all soil types. The parameter sets that are used for the three soil types are presented in Table 1. Note that the distance L between the two canals is chosen differently for each soil type, because surface water features that drain an aquifer are commonly farther apart in aquifers consisting of coarser material. The distance for each soil type is chosen somewhat arbitrarily to allow for a yearly head variation on the order of 1 m.

Evaporation

Evaporation is simulated in the form of transpiration via root uptake; other processes such as interception and soil evaporation are neglected for simplicity. Potential evaporation is distributed over the root depth L_r with a normalized exponential root density function λ (L⁻¹) based on Raats (1974)

$$\lambda(z) = \frac{3}{L_r(1 - \exp(-3))} \exp\left(\frac{3(z - H)}{L_r}\right). \quad (3)$$

Root depth and density are approximated as constant through time.

Actual evaporation E_a is a function of the pressure head ψ and the specified potential evaporation E_p (Feddes et al. 1978). E_a equals zero when the pressure head is below the wilting point ψ_{wp} and equals E_p when the pressure head is above the limiting point ψ_{lp} . E_a varies linearly between the wilting point and the limiting point

$$E_a(\psi) = \begin{cases} E_p & \text{for } \psi > \psi_{lp} \\ \frac{\psi - \psi_{wp}}{\psi_{lp} - \psi_{wp}} E_p & \text{for } \psi_{wp} \leq \psi \leq \psi_{lp} \\ 0 & \text{for } \psi < \psi_{wp} \end{cases}. \quad (4)$$

This root activity function is also visualized in Supporting Information S1. The pressure head for the wilting point is $\psi_{wp} = -10^{4.2} \text{ cm}$. The water content at the limiting point is approximated as constant with a depletion fraction p of 0.5 (Allen et al. 1998)

$$\theta_{lp} = (1 - p)\theta_{fc} + p\theta_{wp}, \quad (5)$$

TABLE 1
Aquifer Parameters for the Three Soil Types.

Soil Type	K_s (mday^{-1})	θ_r (-)	θ_s (-)	α (m^{-1})	β (-)	ε (-)	ψ_b (m)	S_s (m^{-1})	L (m)
Sand	7.128	0.045	0.43	14.5	2.68	3.7548	0.0	10^{-6}	500
Sandy loam	1.061	0.065	0.41	7.5	1.89	4.9540	0.0	10^{-6}	100
Silt loam	0.108	0.067	0.45	2.0	1.41	8.2071	0.0	10^{-6}	50

where θ_{fc} is the field capacity which is approximated as (Twarakavi et al. 2009)

$$\theta_{fc} = \frac{\beta^{-\frac{12}{5}} - \frac{3}{5} \log_{10} K_s}{\theta_s - \theta_r} + \theta_r. \quad (6)$$

Finally, the pressure head for the limiting point ψ_{lp} is computed from θ_{lp} with the inverse of the van Genuchten equation 1.

Modeling Variably Saturated Groundwater Flow

A variety of computer codes is available to model variably saturated groundwater flow. For this study, the MODFLOW USG-Transport code (Panday 2023, Version 2.1.1) is used for a number of reasons. First, the model code is open-source, well-tested, and freely available. Second, the MODFLOW family of codes is flexible and can be used to simulate fairly general groundwater systems. Third, the model uses Newton's method to iteratively obtain a solution for the nonlinear problem, which results in remarkable convergence, even for long time series of daily precipitation and potential evaporation. Convergence of the nonlinear solution is further improved by using the van Genuchten model for the saturation function and the Brooks–Corey model for the hydraulic conductivity. And fourth, the model can be created through Python scripts, making it reproducible and flexible to use (Bakker et al. 2016).

Root uptake is simulated with the EVT package (Harbaugh 2006). Root uptake is not limited when the water content reaches saturation in the current version of the EVT package. To prevent significant root uptake from the saturated zone, the root depth L_r is chosen 0.5 m above the canal stage D such that fully saturated conditions in the root zone do not occur frequently. This is in line with findings of Fan et al. (2017), who report a strong correlation between the root depth L_r and unsaturated zone thickness (i.e., freeboard b).

Weather Data

Daily precipitation and potential (Makkink) evaporation are used for a period of 27 years (1996 through 2022) of which 8 years are shown in Figure 2a as an example. These fluxes are measured by the Royal Netherlands Meteorological Institute (KNMI, 2023) at the meteorological station in Cabauw in The Netherlands where there is a temperate oceanic climate. The mean yearly precipitation rate is 788 mm/year (2.16 mm/day) while the mean precipitation sum on a wet day is 4.31 mm/day (both computed over 1996 through 2023). For a relatively wet year,

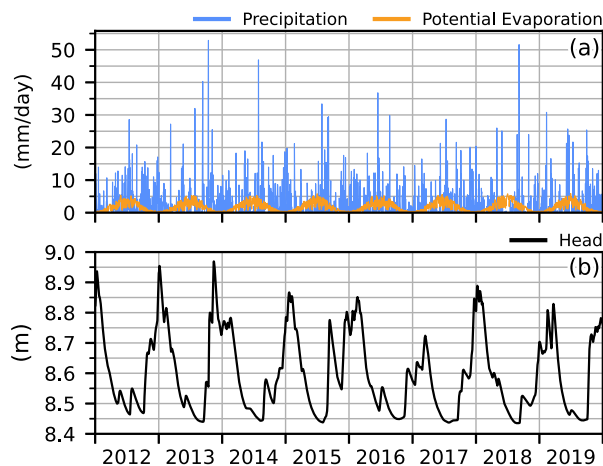


Figure 2. (a) Precipitation (—) and potential (Makkink) evaporation (—) flux from a weather station in Cabauw (Royal Netherlands Meteorological Institute) from January 1, 2012 until December 31, 2019. (b) Synthetic head series (—) from the variably saturated groundwater model for sandy loam with a canal stage D of 8.5 m and a freeboard b of 1.5 m.

such as 2012, the precipitation and evaporation sums are 896 and 599 mm, respectively. For a relatively dry year, such as 2018, these are 637 and 698 mm, respectively.

Numerical Simulation

Three variables are of interest for the numerical simulation of the synthetic head series: the thickness of the unsaturated zone, the soil type, and the location in the model domain. The model domain is discretized in rectangular cells. Fifty-one cells are used in the horizontal direction (cell length is 10 m for sand [$L=500$ m], 2 m for sandy loam [$L=100$ m], and 1 m for silt loam [$L=50$ m]). The grid needs to be finely discretized vertically in the unsaturated zone to obtain an accurate solution. The height of the cells is 0.05 m for the cells potentially in the unsaturated zone: from the surface elevation down to the freeboard b plus 1 m. The cell height is 0.5 m below the freeboard plus 1 m, in the saturated zone, which allows for a faster computation time with no significant loss of accuracy. The number of layers therefore ranges between 56 and 128 for scenarios with $b=1$ and $b=5$ m, respectively. The initial conditions are hydrostatic. The head is computed everyday using the adaptive time-stepping approach of Simunek et al. (2009) as implemented in MODFLOW

USG-Transport. A fully implicit mass conservative solution technique was applied. Although the mass balance error is negligible, slightly different answers may be obtained with different solver settings. This does not significantly affect the conclusions of this article, where the numerical model is used to generate synthetic head series.

Synthetic heads are analyzed for the 20 year period 2003 through 2022, using the 7 years before 2003 as warmup. One 27-year simulation generally takes 30 minutes up to 2 hours, depending on the soil type and non-linearity of the problem (on a regular laptop computer in 2023). The synthetic head represents the water table elevation simulated with the variably saturated model. The water table is the elevation where the pressure head is equal to zero (such that the head is equal to the elevation) and is obtained using linear interpolation in the vertical direction.

An example synthetic head series, created with the variably saturated model, is shown in Figure 2b. The considered soil type is sandy loam with a canal stage $D = 8.5$ m such that the initial unsaturated zone is 1.5 m thick ($b = 1.5$ m). The simulated head varies between 8.4 and 9 m. There are clear peaks in the winters and declines in the summers. The difference between the low heads in a dry summer (2018) and a wet summer (2012) is small for this system and soil type even though the yearly rainfall and potential evaporation amounts are significantly different.

Nonlinear Groundwater Dynamics

In this section, the nonlinearity of the groundwater dynamics for the homogeneous aquifer bounded by two canals (Figure 1) is investigated in detail for all three soil types, and an initial unsaturated zone thickness of 1.5 m ($b = 1.5$ m).

Response to a Precipitation Event Under Constant Infiltration

A linear system is defined here as a groundwater system where the head response is a linear function of the infiltration flux, that is, the head response is twice as large when the infiltration flux is twice as large. Here, it is investigated how much the system under consideration deviates from a linear one. Initially, the system is at a steady state with a constant recharge of 0.5 mm/day, which is approximately equal to the average daily precipitation excess of the precipitation data used in this article. Next, the response to five daily precipitation events of 1, 2, 4, 8, and 16 mm is simulated. Note that the daily sum is doubled for each precipitation event that is simulated.

The head responses to these five precipitation events are shown with solid lines in Figure 3 for the three soil types (one subplot per soil type). The peaks of the responses are different for the three soil types. The peaks are largest for silt loam and smallest for sandy loam (note that the distance L differs for each soil type in Figure 3). The time that it takes for the response to dissipate (also called the memory of the system) depends on the length of the system L and the soil type, but, because the response is nonlinear, also on the precipitation sum. The response time is longest in the sand aquifer and increases from 2207 days (1 mm event) to 2981 days (16 mm event) while for the sandy loam aquifer, the response time varies from 560 to 702 days, and for the silt loam aquifer from 720 to 911 days.

The dashed lines in Figure 3 represent the head response of the 1 mm precipitation event, scaled with the precipitation amount (i.e., the dashed lines represent the response if the system was linear). These dashed lines differ significantly from the actual precipitation responses (solid lines) computed with the model. The peaks of the dashed lines are lower and arrive later. For the sand and sandy loam aquifers, the time difference of the 1 and

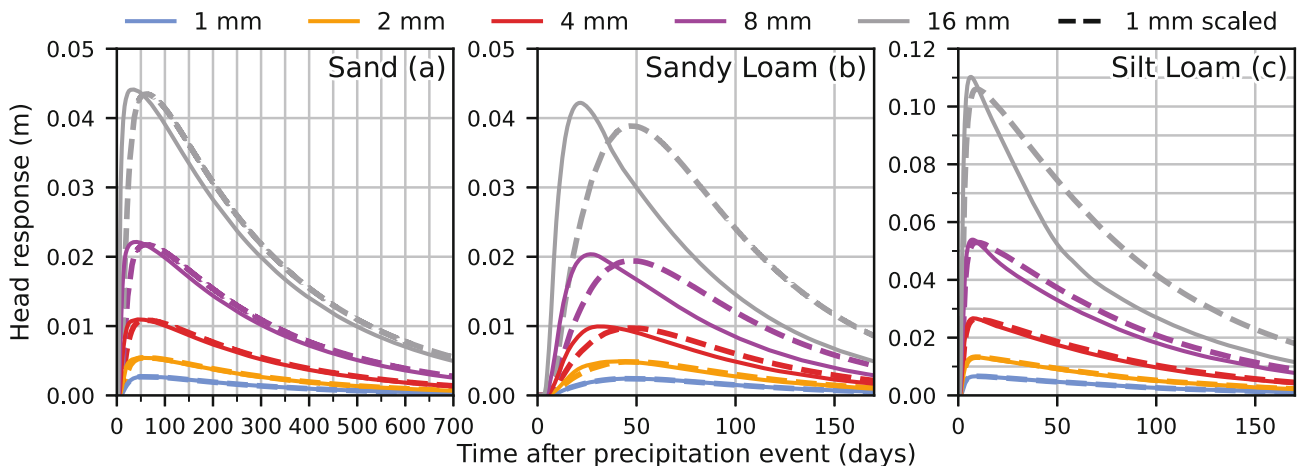


Figure 3. Head response to different precipitation events under constant infiltration at $\frac{x}{L} = 0$ for sand (a), sandy loam (b), and silt loam (c) with a freeboard $b = 1.5$ m. The solid lines show the head response simulated by the variably saturated groundwater model and the dashed lines show the scaled responses from the 1 mm event. Note that the vertical scale is different in the right graph and the horizontal scale is different in the left graph, but the distance between grid lines is the same for all plots.

16 mm peaks is 28.0 and 25.3 days, respectively, while the difference for silt loam is only 2.8 days. The peak arrives earlier and is higher for the actual precipitation responses as compared with the scaled responses because of the sharper wetting front in the unsaturated zone caused by the larger precipitation sum. In summary, it is shown in Figure 3 that the head response to precipitation is nonlinear in that the peak of the response and the response time depend in a nonlinear fashion on the magnitude of the precipitation event.

Response to a Precipitation Event Under Time-Varying Conditions

In reality, the system is never at a steady state with a constant infiltration rate and the head response happens during conditions resulting from highly variable meteorological stresses. Infiltration rates may show daily, seasonal, annual, and multi-annual patterns, resulting in highly variable water content in the unsaturated zone. The previous example is repeated but then for a one-day precipitation event of 4 mm (the average precipitation sum on a wet day for the data used in this article) added to the actual precipitation and potential evaporation rates. The head response is computed as the difference between the simulated head with the added daily event of 4 mm and the simulated head without the added event. The response is computed for six events in 2015 (arbitrarily chosen across the year to show different responses). To illustrate the effect of the unsaturated zone, the head response is also simulated with a model without an unsaturated zone, that is, only unconfined saturated flow. This unconfined model uses a specific yield $S_y = \theta_s - \theta_{fc}$. The results for the unconfined model (only saturated flow) are plotted in Figure 4a and the results for the variably saturated groundwater model are plotted in Figure 4b.

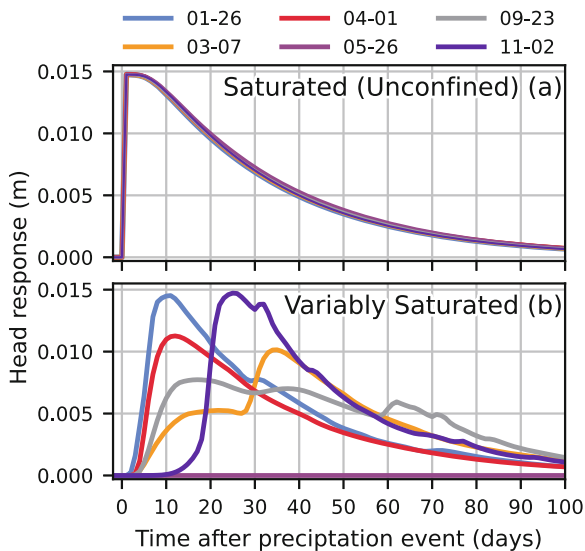


Figure 4. Head response to 4 mm (extra) precipitation on selected dates (MM-DD) in 2015 at $\frac{x}{L} = 0$ for a saturated (unconfined) groundwater model at $z = 0$ (a) and head response in the variably saturated groundwater model (with a freeboard of 1.5 m) (b). The soil type is sandy loam.

The nonlinear effect of the unsaturated zone on the head response is clearly visible in the differences between the results shown in Figure 4a and 4b. The head responses for the six events are similar in the unconfined model (no unsaturated zone); small variations can only be caused by the time-varying thickness of the saturated zone. In contrast, the head responses for the six events in the variably saturated groundwater model vary widely (Figure 4b). For the event on 05-26 (purple line) there is no response at all, meaning that all precipitation evaporated. For other responses (e.g., orange line on 03-07), there are two peaks. These secondary peaks can be explained by the higher saturation degree in the unsaturated zone due to this 4 mm precipitation event. As a result of the higher saturation, a precipitation event that happens at a later time can arrive quicker at the water table. In summary, the majority of the nonlinear head response simulated by the groundwater model stems from the unsaturated zone, while the nonlinearity resulting from the varying thickness of the saturated zone is negligible for the chosen model setup.

Time Series Model

In this section, the time series model is described. The description is kept concise; additional details may be found in the given references. The time series model is implemented in the open-source Python package Pastas (Collenteur et al. 2019, Version 1.3.0). The performance of the time series models to simulate the synthetic head series generated earlier is discussed in the next section.

The basic time series model is the same for both the linear and nonlinear recharge models. The head response to recharge, the basic time series model, is obtained through convolution as

$$h(t) = \int_{-\infty}^t R(\tau)\vartheta(t - \tau)d\tau + d + r(t), \quad (7)$$

where h is the time series of head observations (L), R (L/T) is the time series of recharge, ϑ is the impulse response function for recharge, d is the base elevation of the model (L), and r are the residuals (L). The impulse response function used here is the scaled Gamma function, which is a versatile function that gives a good fit in many circumstances

$$\vartheta(t) = \frac{A}{a^n \Gamma(n)} t^{n-1} \exp(-t/a), \quad (8)$$

where A , a , and n are shape parameters and Γ is the Gamma function. An example of the scaled Gamma function is added to Supporting Information S1.

For the linear recharge model, the recharge R is a linear combination of the precipitation P and potential evaporation E_p

$$R(t) = P(t) + fE_p(t), \quad (9)$$

where f is a negative parameter called the evaporation factor (Oberfell et al. 2019) scaling the potential

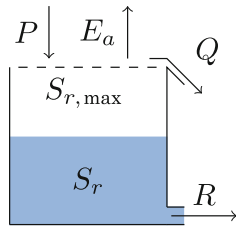


Figure 5. Schematic representation of the nonlinear recharge model using a root zone reservoir.

evaporation. The recharge flux can be negative or positive depending on the precipitation and evaporation fluxes; a negative recharge is a rudimentary representation of capillary rise. The linear time series model has five parameters: the shape parameters A , n , a of the scaled Gamma response function, the base elevation d , and the evaporation factor f .

For the nonlinear recharge model, the model adopted by Collenteur et al. (2021) is used. The model is shown schematically in Figure 5. The model stores water S_r (L) in a root zone reservoir with maximum storage $S_{r,max}$ (L). The water balance for the root zone reservoir is written as

$$\frac{dS_r}{dt} = P(t) - E_a(t) - R(t) - Q(t), \quad (10)$$

where P (L/T) is the precipitation flux, E_a (L/T) is the actual evaporation flux, R (L/T) is the recharge flux, and Q (L/T) is the runoff flux. The actual evaporation flux is expressed as

$$E_a(t) = k_v E_p(t) \min\left(1, \frac{S_r(t)}{l_p S_{r,max}}\right), \quad (11)$$

where E_p (L/T) is the given potential evaporation flux and k_v (–) is a vegetation coefficient. Parameter l_p (–) determines at what fraction of the maximum root zone storage the evaporation flux is limited by the availability of water. Recharge from the root zone reservoir is calculated as

$$R(t) = C \left(\frac{S_r(t)}{S_{r,max}} \right)^\gamma, \quad (12)$$

where C (L/T) is a conductivity term, and γ (–) is a parameter that determines how nonlinear the recharge flux is with respect to the storage in the root zone reservoir. In contrast to the linear mode, the recharge flux can only be positive, which means that capillary rise cannot be simulated. Runoff is simulated when the root zone storage exceeds the maximum root zone storage

$$Q(t) = \max(0, P(t) - (S_{r,max} - S_r(t))). \quad (13)$$

The nonlinear time series model has the same four parameters A , n , a , and d as the linear model, plus the parameters $S_{r,max}$, k_v , l_p , C , and γ .

The parameters of the times series model are estimated by minimizing the sum of the squared normalized residuals using a standard nonlinear least squares routine. The normalized residuals are computed as the residuals minus the mean of the residuals. The parameter d is not fitted but set equal to the mean of the residuals after optimization is completed. The parameters of the nonlinear recharge model can be difficult to estimate independently because they are highly correlated with the maximum storage. $S_{r,max}$ is therefore set equal to $S_{r,max} = 0.1b$. Parameter k_v is set to 1 because the potential evaporation is known (as specified in the variably saturated groundwater model). The parameter l_p is set to 0.25 (Collenteur et al. 2021). As a result, the number of parameters to be estimated for the linear model is four (A , a , n , f) and the number of parameters to be estimated for the nonlinear model is five (A , a , n , C , and γ).

Performance Assessment

All models are assessed using three goodness-of-fit metrics: the coefficient of determination (R^2), the root mean squared error (RMSE), and the mean absolute error (MAE). The R^2 gives a good indication of the success in covering the variability of the observations and ranges between $-\infty$ and 1 of which the latter indicates perfect agreement between the observed and simulated values. An $R^2 \leq 0$ means that the average head is a better model than the simulated heads. The equation for R^2 is (Wright 1921)

$$R^2 = 1 - \frac{\sum (h - h_s)^2}{\sum (h - \bar{h})^2}, \quad (14)$$

where h is the observed head (in this case the synthetic head series), \bar{h} is the mean observed head, and h_s is the simulated head (by the time series model); the summation is over the number of observations. The RMSE and MAE are only reported in Supporting Information S1 since they are less useful when comparing the model performance for head series with different total head variations.

Results

The described procedure for numerical simulation of the synthetic head series was applied to generate series for three soil types (sand, sandy loam, and silt loam), nine freeboards $b \in \{1, 1.5, \dots, 5\}$, and five locations in the model domain $\frac{x}{L} \in \{0, \frac{1}{10}, \frac{1}{5}, \frac{3}{10}, \frac{2}{5}\}$. This results in a total of 135 synthetic series. The linear and nonlinear models were tested for all 135 series. The time series model is calibrated for the 13 year period (2003 through 2015) using the 7 years before 2003 as warmup. The 7 year period 2016 through 2022 is used as a validation period. In the following, the results are first presented in detail for a thick and a thin unsaturated zone, after which the results of all 135 models are analyzed.

Analysis of Selected Synthetic Series

The model performance for six synthetic head series is shown in Figure 6. Daily values of synthetic heads are simulated halfway between the two canals ($\frac{x}{L} = 0$). For

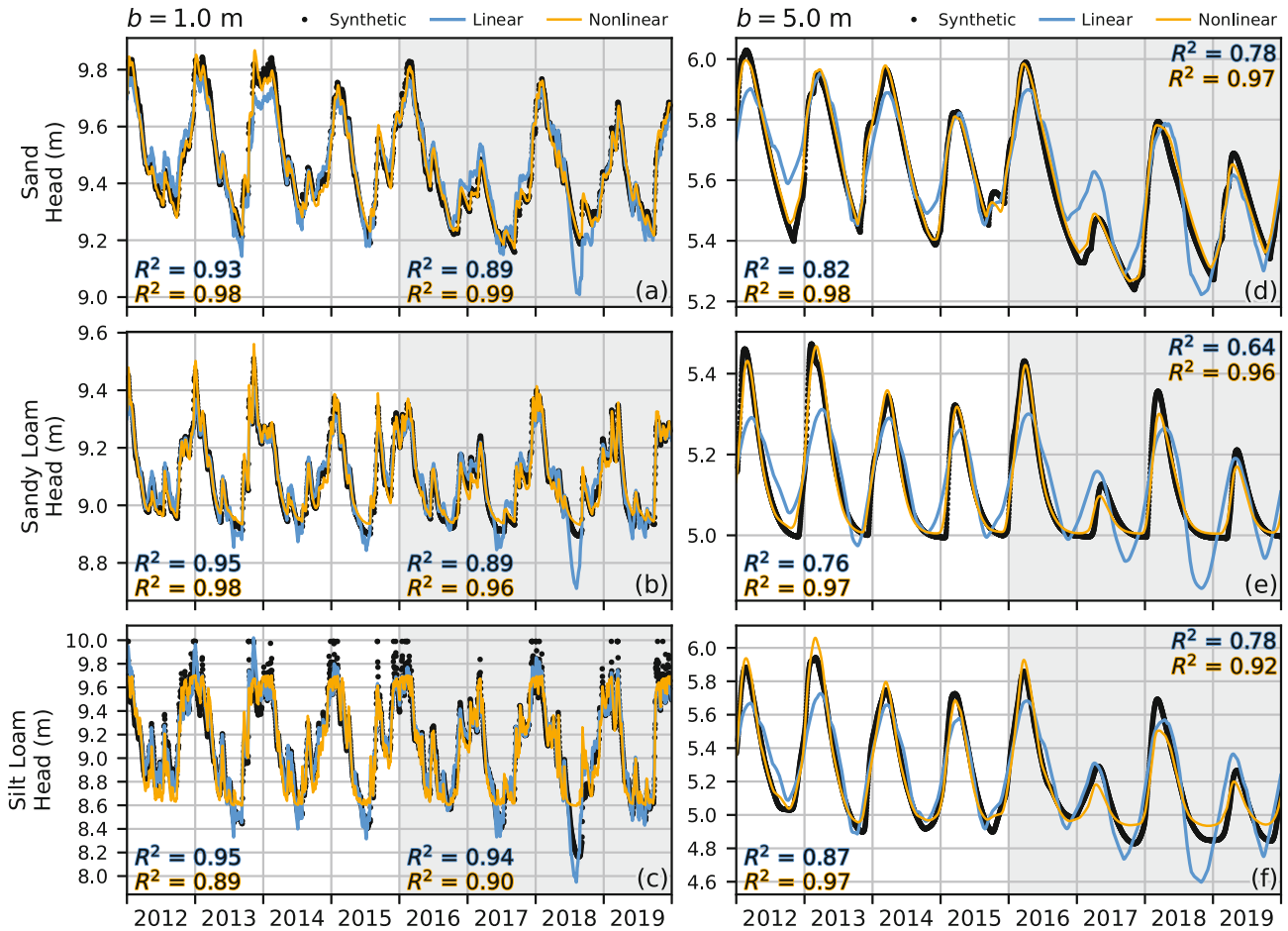


Figure 6. Example of generated synthetic heads at $\frac{x}{L} = 0$ (. . .) and fitted linear (—) and nonlinear (—) time series models for three soil types (rows) and for a thin unsaturated zone (left column) and a thick unsaturated zone (right column). Eight years from January 1, 2012 until December 31, 2019 are shown of which the first four (2012 through 2015) are in the calibration period and the last four (2016 through 2019) are in the validation period denoted by the gray background. The coefficient of determination R^2 of the linear and nonlinear model is reported for the shown parts of the calibration and validation periods. Note that the vertical scale differs for each graph, but the difference between two horizontal grid lines is 0.2 m for all graphs.

illustration purposes, only the period 2012 through 2019 is shown. Each row represents one of the three soil types. The left column is for a thin unsaturated zone (freeboard $b = 1$ and canal stage $D = 9$ m) while the right column is for a thick unsaturated zone ($b = 5$ m and $D = 5$ m). The synthetic heads are shown with black dots Results are shown for both the linear recharge model (blue —) and the nonlinear recharge model (yellow —). The R^2 values presented in Figure 6 are for the 4 years of the calibration period and the 4 years of the validation period that are shown in the figure.

Groundwater dynamics for a thin unsaturated zone (small freeboard as in left column) are significantly different compared with a thick unsaturated zone (large freeboard as in right column). Note that the vertical scale differs between graphs in Figure 6, as the total head variation differs significantly, but the tick marks on the vertical axis are every 0.2 m for all graphs to facilitate comparison. Also recall that the distance between the canals L changes with the soil type, which explains some

of the difference in total head variation between soil types. The head variation is much flashier for the thin unsaturated zone and the total head variation is larger than the head variation for the thick unsaturated zone (for the same soil type), as a thicker unsaturated zone smooths both the wetting front in the unsaturated zone and the resulting recharge flux that reaches the water table.

For the thin unsaturated zone (left column), the heads drop below the water level in the canals (9 m) during the summers for the sandy loam and silt loam. This means that water flows from the water table into the unsaturated zone (capillary rise), which implies that water is flowing from the left and right boundaries to the middle of the aquifer. For the thick unsaturated zone (right column), the head drops below the water level in the canal (5 m) for the silt loam only. For silt loam, the drop below the canal level is approximately 80 cm for the thin unsaturated zone, but is at most 20 cm for the thicker unsaturated zone.

The fit of both the linear and nonlinear model is relatively high for all three soils with a thin unsaturated zone (left column of Figure 6) as the R^2 is 0.88 or higher for all models in both the calibration and validation periods. The performance of the nonlinear model is better than the linear model for sand and sandy loam, but the difference is small. For silt loam, the linear model performs better than the nonlinear model ($R^2 = 0.95/0.94$ vs. $R^2 = 0.89/0.90$), especially in simulating the low heads in the summers.

For the thick unsaturated zone (right column of Figure 6), the performance of the nonlinear model is very good as the R^2 is close to 1 in the calibration period with only a slightly smaller value in the validation period. The nonlinear model performs substantially better than the linear model for the thick unsaturated zone for all three soils. Note that the heads simulated with the linear model are too low in the dry summer of 2018 for all models shown in Figure 6, while the nonlinear model gives more accurate results.

Analysis of All Synthetic Series

The performance of the linear and nonlinear models is summarized for all 135 synthetic head series in Figure 7. Each subplot shows the model performance expressed as the coefficient of determination R^2 for the calibration period (2003 through 2015) and the validation period (2016 through 2022). The line represents the

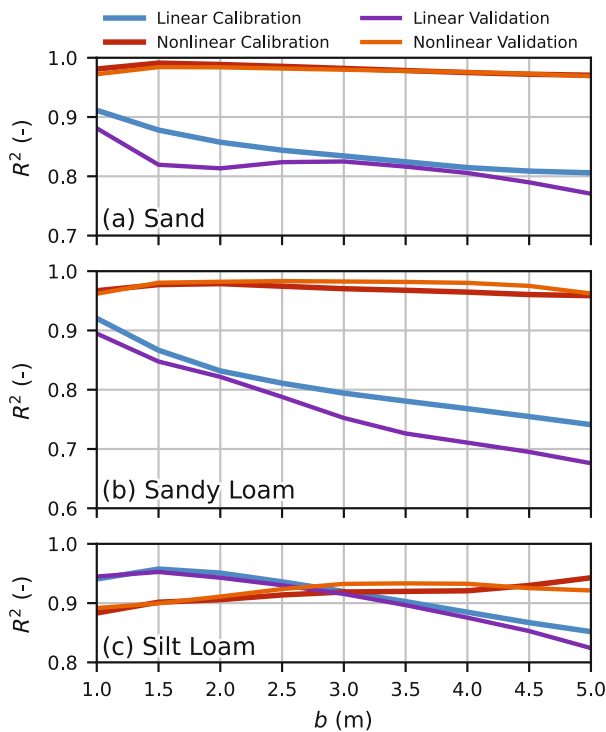


Figure 7. The coefficient of determination (R^2) averaged over all locations as a function of the freeboard for sand (a), sandy loam (b), and silt loam (c). Results are shown for the calibration period (2002 through 2015) and the validation period (2016 through 2022) for both the linear and nonlinear model.

average performance over all five locations $\frac{x}{L}$ in the model domain since the differences in value of the goodness-of-fit metrics per location were generally small. The blue (—) and purple (—) colors are used for the linear models and the red (—) and orange (—) colors for the nonlinear models. One graph is shown for each of the three soil types and for a freeboard varying from $b = 1$ m (thin unsaturated zone) to $b = 5$ m (thick unsaturated zone). Note that the models of Figure 6 are for $b = 1$ (left column) and $b = 5$ (right column) and for $\frac{x}{L} = 0$ only. Similar figures for the performance metrics MAE and RMSE and tables with the metrics for all models can be found in Supporting Information S1.

The nonlinear model generally performs well with R^2 values above 0.9 for most models. The performance of the linear models is lower than the nonlinear models, with an R^2 below 0.9 for most models, and below 0.8 for many sandy loam models. The performance of the nonlinear model does not differ much between thinner (small b) and thicker (large b) unsaturated zones. The performance of the linear model generally decreases with the thickness of the unsaturated zone (larger b). The linear model only performs better than the nonlinear model for silt loam with thin unsaturated zones ($b < 3$ m). This coincides with synthetic head series where the head drops far below the canal stage, indicating capillary rise.

Head Response of the Time Series Models

So far, model performance was assessed using the goodness-of-fit metric R^2 for both the calibration and validation periods. The validation period consists of an independent check, as the heads in the validation period were not used during calibration. In addition, it is preferable to assess model performance with other independent data or responses when possible. For example, Collenteur et al. (2021) compared the simulated recharge flux of their nonlinear time series model with measured lysimeter seepage. Here, the head response of the time series model is compared with the head response of the numerical model (i.e., “the truth”) used to simulate the synthetic heads. The response of six daily precipitation events of 4 mm in 2015 was simulated previously with the numerical model for sandy loam with a freeboard of 1.5 m (Figure 4b).

The head response to the same six precipitation events is simulated with the calibrated linear (dashed lines) and nonlinear (dashdotted lines) time series models and are shown in Figure 8. The head response of the linear time series model is the same for all six events. The responses simulated with the nonlinear time series model are similar to the “true” responses. This is shown by the multiple peaks with the responses of 03-07 (orange —) and 09-22 (gray —) or no response at 05-26 (purple —). The similarity between the head responses of the nonlinear time series model and the variably saturated groundwater model suggests that the nonlinear time series model is getting the right answer for the right reasons (e.g., Kirchner 2006).

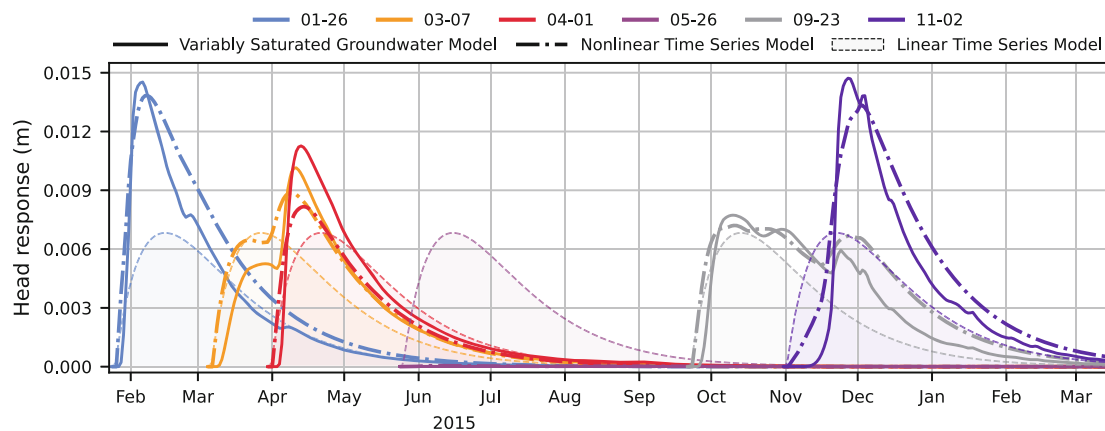


Figure 8. Head response to 4 mm (extra) precipitation on selected dates (MM-DD) in 2015 for the nonlinear time series model (---) and the linear time series model (···) compared with the corresponding head response of the variably saturated groundwater model (—, same as Figure 4b). The response is shown for sandy loam at $\frac{x}{L} = 0$ with a freeboard of 1.5 m.

Discussion

The main objective of this article is to test nonlinear time series models by applying them to synthetic head series generated with a variably saturated zone model where both the physics of the problem and the input series (precipitation and potential evaporation) are fully known. In this section, the generation of realistic synthetic head series is revisited first, followed by the nonlinear recharge model. The implications for time series analysis are discussed at the end of this section.

Generating Realistic Synthetic Head Series

It was attempted to create realistic synthetic head series while keeping the complexity of the model manageable. The van Genuchten equation 1 was used to describe the water content as a function of the pressure head while the Brooks–Corey function (Equation 2) was used to describe the hydraulic conductivity as a function of the pressure head (e.g., Fuentes et al. 1992). This combination of van Genuchten for $\theta(\psi)$ and Brooks–Corey for $K(\psi)$ may be less common, but significantly improves the convergence of the nonlinear solution of Richards' equation for this study. Evaporation is simulated as transpiration via root uptake. Root water uptake was distributed over the constant root zone thickness using an exponential root zone density function (Equation 3). This model results in useful synthetic series even though not all complexities of realworld systems are included.

Many approximations had to be made to keep the scope of the article manageable. The main approximations are the following:

- The aquifer properties are homogeneous and preferential flow is not included.
- Meteorological stresses are used from a temperate oceanic climate. Precipitation and potential evaporation are averaged over a day and are applied uniformly along the horizontal direction. No errors or noise are added to the precipitation and evaporation series.

- Runoff is removed from the model rather than fed back to the system (e.g., through ponding or overland flow to the canals).
- The canal stage is kept constant. The left and right boundary conditions above the water table are hydrostatic rather than a seepage face.
- The root depth is constant through time (no root growth). Root water uptake is not limited when the soil is fully saturated.
- Interception and soil evaporation are not included.
- No random errors are added to the generated head series to represent for example measurement error or other uncertainties.

The variably saturated groundwater model (MODFLOW USG-Transport) and the Python scripts that were used to run the model can be accessed publicly via Zenodo (Vonk et al. 2024). As a result, any complexity or process that was not included but is deemed important can be added in future research.

Nonlinear Recharge Model

The main feature of the nonlinear recharge model is that both recharge and evaporation are based on the available storage in the root zone reservoir. As a result, actual evaporation is less than potential evaporation when the storage in the root zone reservoir is low. This is called evaporation reduction. The degree of evaporation reduction depends on factors such as the soil type, root distribution, and potential evaporation. Finer-grained soils exhibit less evaporation reduction compared with coarser-grained soil types because finer-grained soils offer greater water availability at lower pressure heads. Evaporation reduction is not included in the linear recharge model. The effect of omission of evaporation reduction can clearly be seen in Figure 6 where for a dry summer such as 2018 the linear model significantly undershoots the observed (synthetic) heads. Such undershoots by linear models in dry summers are also reported in practice by, for example, Berendrecht et al. (2006), Peterson and Western (2014), and Collentur et al. (2021).

Capillary rise causes water flow from the water table into the root zone and can be considerable (e.g., Raats 1974; Kroes et al. 2018). From the root zone, this water may in turn be transpired by plants. Capillary rise is not included in the nonlinear recharge model used in this article (Figure 5). Capillary rise is more pronounced in finer-grained soils than in coarser-grained soils and is more pronounced in thin unsaturated zones than in thick unsaturated zones. For silt loam and a thin unsaturated zone (Figure 6c), capillary rise is significant (the head drops more than 0.8 m below the canal stage D of 9 m). The linear model is quite capable of simulating this behavior, but the nonlinear model is not.

The nonlinear time series model performs quite well for the cases considered in this article, except for fine grained material in combination with a thin unsaturated zone (Figure 6). For this latter case, the nonlinear time series model cannot simulate the peaks (which are capped by the ground surface) or the valleys in the synthetic head series. The valleys cannot be simulated because the nonlinear model cannot simulate capillary rise, as mentioned above. The peaks cannot be simulated because the nonlinear recharge model does not cap heads at the ground surface, but caps the storage in the root zone reservoir when the maximum storage $S_{r,max}$ is reached.

The nonlinear time series model seems to give the right answer for the right reason, as the simulated response of the nonlinear recharge model in combination with a Gamma response function is similar to the response of the variably saturated model (Figure 8). Even though this is encouraging, significant improvements are needed for certain cases. The nonlinear recharge model needs to be modified to include the possibility of capillary rise and capping of groundwater levels at the ground surface. The nonlinear recharge model currently includes five parameters, some of which are highly correlated. This means that some parameters have to be fixed to be able to obtain a solution (Collenteur et al. 2021). Modifications are needed such that all parameters in the model can be estimated. Alternatively, it could be investigated if the size of the root zone reservoir can be estimated using other methods (e.g., Gao et al. 2014).

Implications for Time Series Modeling

The results from this study clearly show that groundwater dynamics are nonlinear because of flow processes in the unsaturated zone. The head response to a single precipitation event varies significantly depending on the saturation of the root zone, and ultimately the precipitation and evaporation that occurs both before and after the precipitation event (Figures 3 and 4). In that respect, it is somewhat surprising how well the linear recharge model performs even though it uses a single response function that is only scaled by the precipitation amount. For example, the response function of the linear model for sandy loam and a freeboard of 1.5 (the dashed lines in Figure 8) results in an R^2 above 0.85 even though the actual response functions (for example the solid lines

in Figure 8) can be vastly different. The fit of the linear model in the validation period is generally somewhat lower than in the calibration period, which is an indication of mild overfitting. Apparently, the effect of a sequence of daily precipitation and evaporation averages out over time, resulting in a fairly good performance for many head series in systems with shallow water tables, as also reported in practice for large datasets by Zaadnoordijk et al. (2019) and Brakenhoff et al. (2022). It can be expected that a nonlinear model would further improve these results, as it includes significant physical processes that are not included in the linear model. Other recent studies from the Baltics (Jemeljanova et al. 2023) and Switzerland (Collenteur et al. 2023), where such systematic comparisons were performed, showed that nonlinear models often outperform the linear approximation, but not for all monitoring wells.

Conclusions

The numerical groundwater model MODFLOW USG-Transport was used to simulate synthetic head series for variably saturated flow between two parallel canals, where daily variations of precipitation and potential evaporation were specified at the land surface. The head response was simulated in a homogeneous unconfined aquifer for three different soil types varying from sand to silt loam; root water uptake was simulated. The numerical simulations clearly demonstrated the (well-known) nonlinear head response of a system when the unsaturated zone is included.

Synthetic heads were simulated for a period of 27 years of daily precipitation and potential evaporation, for three different soil types and for seven freeboards varying from 1 to 5 m. (i.e., the thickness of the unsaturated zone varied between 0 to more than 5 m during simulation). The synthetic heads were used to assess the performance of both a linear and a nonlinear time series model. No additional errors were introduced to either the synthetic head series or to the input series (precipitation and potential evaporation), so any mismatch was the result of model structural error.

The recharge in the linear model is simulated as a linear function of the precipitation and potential evaporation, while the recharge in the nonlinear model is simulated with a root zone reservoir where both the recharge and actual evaporation are a function of the water stored in the reservoir. The nonlinear time series model outperformed the linear time series model for almost all synthetic head series in both the calibration and validation periods. After the calibration, the nonlinear time series model was used to simulate the response to a 1-day precipitation event at different times during the year. The response simulated with the nonlinear time series model was very similar to the response simulated with the variably saturated model used to simulate the synthetic head series. This demonstrates that the inclusion of important nonlinear processes improves the model. On the other hand, the nonlinear time series model did not

perform as well for the cases where capillary rise played a significant role, which is a process that is not included in the nonlinear time series model.

Although the performance of the linear model was not as good as the nonlinear model, the performance was good (R^2 above 0.8) for quite a few settings, especially for thinner unsaturated zones. On the one hand, this is not a surprise as several studies have reported successful application of linear time series models in aquifers with shallow water tables (e.g., von Asmuth et al. 2002; Zaadnoordijk et al. 2019), but it is somewhat surprising considering that the linear model uses one average response function (e.g., the dashed lines in Figure 8) while the head response varies wildly throughout a year (Figure 4).

A clear implication of this work is that nonlinear time series models deserve to be used more often, and can be expected to perform better than the linear model in many real-life applications. Nonlinear time series models are ready for application in practice, but additional testing and development are required. For example, it needs to be investigated how nonlinear models perform in heterogeneous aquifers and arid, tropical, or continental climates instead of the temperate oceanic climate considered in this article. It was shown in this article that time series models improved significantly through the inclusion of some nonlinear processes. The inclusion of other processes such as capillary rise is the topic of future research.

Substantial effort went into the development of an open-source, reproducible, and scripted workflow to generate synthetic head series with an open-source groundwater model with variably saturated flow (Vonk et al. 2024). The stable performance of the open-source MODFLOW USG-Transport code to simulate the groundwater dynamics for many years of daily precipitation and potential evaporation is quite remarkable. The developed workflow can benefit other developers to test their (data-driven) models in controlled numerical experiments.

Acknowledgments

The authors thank Chris Nicol, David Brakenhoff, Ruben Caljé, and Onno Ebbens for answering questions regarding MODFLOW (USG-Transport), FloPy, and Pastas.

Data Availability Statement

The (scripted) workflow to generate synthetic head data and perform the time series analysis can be found on an online repository: Vonk et al. (2024).

Supporting Information

Additional supporting information may be found online in the Supporting Information section at the end of the article. Supporting Information is generally *not* peer reviewed.

Supporting Information S1. The supporting information has five sections: *Soil Hydraulic Properties* with figures of the soil water retention curves and hydraulic conductivity function of the three soil types used in this article. *Root Activity Function* with a figure of the root activity function described by Equation 4. *Scaled Gamma Response* with a figure of an example of the response function described by Equation 8. *Goodness-of-Fit Metrics* with figures of the RMSE and MAE and tables with all metrics for all time series models. *Optimized Time Series Model Parameters* with tables for the optimized parameters for all time series models found by the least squares algorithm.

References

- Allen, R.G., L.S. Pereira, D. Raes, and M. Smith. 1998. Crop evapotranspiration – Guidelines for computing crop water requirements. In: FAO Irrigation and Drainage Paper. Vol. 56, Ch. 8, Food and Agriculture Organization of the United Nations, Rome, Italy.
- Bakker, M., and F. Schaars. 2019. Solving groundwater flow problems with time series analysis: You may not even need another model. *Groundwater* 57, no. 6: 826–833. <https://doi.org/10.1111/gwat.12927>
- Bakker, M., V. Post, C.D. Langevin, J.D. Hughes, J.T. White, J.J. Starn, and M.N. Fienen. 2016. Scripting MODFLOW model development using Python and FloPy. *Groundwater* 54, no. 5: 733–739. <https://doi.org/10.1111/gwat.12413>
- Bakker, M., K. Maas, and J.R. von Asmuth. 2008. Calibration of transient groundwater models using time series analysis and moment matching. *Water Resources Research* 44, no. 4: W04420. <https://doi.org/10.1029/2007WR006239>
- Bakker, M., K. Maas, F. Schaars, and J.R. von Asmuth. 2007. Analytic modeling of groundwater dynamics with an approximate impulse response function for areal recharge. *Advances in Water Resources* 30, no. 3: 493–504. <https://doi.org/10.1016/j.advwatres.2006.04.008>
- Berendrecht, W.L., F.C. van Geer, J.C. Gehrels, and A.W. Heemink. 2006. A non-linear state space approach to model groundwater fluctuations. *Advances in Water Resources* 29, no. 7: 959–973. <https://doi.org/10.1016/j.advwatres.2005.08.009>
- Brakenhoff, D.A., M.A. Vonk, R.A. Collenteur, M. van Baar, and M. Bakker. 2022. Application of time series analysis to estimate drawdown from multiple well fields. *Frontiers in Earth Science* 10: 907609. <https://doi.org/10.3389/feart.2022.907609>
- Brooks, R.H., and A.T. Corey. 1964. Hydraulic properties of porous media. In: Hydrology Papers 3, Fort Collins, Colorado State University, Colorado.
- Carsel, R.F., and R.S. Parrish. 1988. Developing joint probability distributions of soil water retention characteristics. *Water Resources Research* 24, no. 5: 755–769. <https://doi.org/10.1029/WR024i005p00755>
- Collenteur, R.A., M. Bakker, G. Klammler, and A. Birk. 2021. Estimation of groundwater recharge from groundwater levels using nonlinear transfer function noise models and comparison to lysimeter data. *Hydrology and Earth System Sciences* 25, no. 5: 2931–2949. <https://doi.org/10.5194/hess-25-2931-2021>
- Collenteur, R.A., C. Moeck, M. Schirmer, and S. Birk. 2023. Analysis of nationwide groundwater monitoring networks using lumped-parameter models. *Journal of Hydrology* 626: 130120. <https://doi.org/10.1016/j.jhydrol.2023.130120>
- Collenteur, R.A., M. Bakker, R. Caljé, S.A. Klop, and F. Schaars. 2019. Pastas: Open source software for the

- analysis of groundwater time series. *Groundwater* 57, no. 6: 877–885. <https://doi.org/10.1111/gwat.12925>
- Fan, Y., G. Miguez-Macho, E.G. Jobbgy, R.B. Jackson, and C. Otero-Casal. 2017. Hydrologic regulation of plant rooting depth. *Proceedings of the National Academy of Sciences* 114, no. 40: 10572–10577. <https://doi.org/10.1073/pnas.1712381114>
- Feddes, R.A., P. Kabat, P.J.T. van Bakel, J.J.B. Bronswijk, and J. Halbertsma. 1988. Modelling soil water dynamics in the unsaturated zone – state of the art. *Journal of Hydrology* 100, no. 1: 69–111. [https://doi.org/10.1016/0022-1694\(88\)90182-5](https://doi.org/10.1016/0022-1694(88)90182-5)
- Feddes, R.A., P.J. Kowalik, and H. Zaradny. 1978. *Simulation of Field Water Use and Crop Yield*. New York: John Wiley & Sons.
- Fuentes, C., R. Haverkamp, and J.Y. Parlange. 1992. Parameter constraints on closed-form soilwater relationships. *Journal of Hydrology* 134, no. 1: 117–142. [https://doi.org/10.1016/0022-1694\(92\)90032-Q](https://doi.org/10.1016/0022-1694(92)90032-Q)
- Gao, H., M. Hrachowitz, S.J. Schymanski, F. Fenicia, N. Sriwongsitanon, and H.H.G. Savenije. 2014. Climate controls how ecosystems size the root zone storage capacity at catchment scale. *Geophysical Research Letters* 41, no. 22: 7916–7923. <https://doi.org/10.1002/2014GL061668>
- Harbaugh, A.W. 2006. MODFLOW-2005, the U.S. Geological Survey modular ground-water model—the ground-water flow process. Techniques and Methods. Vol. 6-A16, U.S. Geological Survey. <https://doi.org/10.3133/tm6A16>.
- Hunt, R.J., D.E. Prudic, J.F. Walker, and M.P. Anderson. 2008. Importance of unsaturated zone flow for simulating recharge in a humid climate. *Groundwater* 46, no. 4: 551–560. <https://doi.org/10.1111/j.1745-6584.2007.00427.x>
- Jemeljanova, M., R.A. Collenteur, A. Kmoch, J. Bike, K. Popovs, and A. Kalvans. 2023. Modeling hydraulic heads with impulse response functions in different environmental settings of the Baltic countries. *Journal of Hydrology: Regional Studies* 47: 101416. <https://doi.org/10.1016/j.ejrh.2023.101416>
- Kirchner, J.W. 2006. Getting the right answers for the right reasons: Linking measurements, analyses, and models to advance the science of hydrology. *Water Resources Research* 42, no. 3: W03S04. <https://doi.org/10.1029/2005WR004362>
- Klop, S.A. 2019. From observation well to model area: Estimating groundwater levels spatially using time series analysis. Master's thesis, Delft University of Technology, The Netherlands.
- Kroes, J., I. Supit, J. van Dam, P. van Walsum, and M. Mulder. 2018. Impact of capillary rise and recirculation on simulated crop yields. *Hydrology and Earth System Sciences* 22, no. 5: 2937–2952. <https://doi.org/10.5194/hess-22-2937-2018>
- Niswonger, R. G., D. E. Prodic, and R. S. Regan. 2006. Documentation of the unsaturated-zone flow (UZFI) package for modeling unsaturated flow between the land surface and the water table with MODFLOW-2005. Techniques and Methods, Vol. 6-A19, U.S. Geological Survey. <https://doi.org/10.3133/tm6A19>.
- Obergfell, C., M. Bakker, and K. Maas. 2019. Estimation of average diffuse aquifer recharge using time series modeling of groundwater heads. *Water Resources Research* 55, no. 3: 2194–2210. <https://doi.org/10.1029/2018WR024235>
- Panday, S. 2023. USG-transport: Transport and other enhancements to MODFLOW-USG. Version: 2.1.1. GSI Environmental. <https://www.gsienv.com/product/modflow-usg/>.
- Peterson, T.J., and A.W. Western. 2014. Nonlinear time-series modeling of unconfined groundwater head. *Water Resources Research* 50, no. 10: 8330–8355. <https://doi.org/10.1002/2013WR014800>
- Raats, P.A.C. 1974. Steady flows of water and salt in uniform soil profiles with plant roots. *Soil Science Society of America Journal* 38, no. 5: 717–722. <https://doi.org/10.2136/sssaj1974.03615995003800050012x>
- Richards, L.A. 1931. Capillary conduction of liquids through porous mediums. *Physics* 1, no. 5: 318–333. <https://doi.org/10.1063/1.1745010>
- Romano, N., M. Palladino, and G.B. Chirico. 2011. Parameterization of a bucket model for soil-vegetation-atmosphere modeling under seasonal climatic regimes. *Hydrology and Earth System Sciences* 15, no. 12: 3877–3893. <https://doi.org/10.5194/hess-15-3877-2011>
- Royal Netherlands Meteorological Institute (KNMI). 2023. Dagwaarden van weerstations. <https://daggegevens.knmi.nl/klimatologie/daggegevens>.
- Shapoori, V., T.J. Peterson, A.W. Western, and J.F. Costelloe. 2015. Decomposing groundwater head variations into meteorological and pumping components: A synthetic study. *Hydrogeology Journal* 23, no. 7: 1431–1448. <https://doi.org/10.1007/s10040-015-1269-7>
- Siegel, D.I., and E.J. Hinchey. 2019. Big data and the curse of scale. *Groundwater* 57, no. 4: 505. <https://doi.org/10.1111/gwat.12905>
- Simunek, J., M. Sejna, H. Saito, M. Sakai, and M.Th. van Genuchten. 2009. *The HYDRUS-1D software package for simulating the one-dimensional movement of water, heat, and multiple solutes in variably-saturated media. Version 4.08*. Riverside, CA: Department of Environmental Sciences, University of California, Riverside.
- Twarakavi, N.K.C., M. Sakai, and J. Simunek. 2009. An objective analysis of the dynamic nature of field capacity. *Water Resources Research* 45, no. 10: W10410. <https://doi.org/10.1029/2009WR007944>
- van Genuchten, M.Th. 1980. A closed-form equation for predicting the hydraulic conductivity of unsaturated soils. *Soil Science Society of America Journal* 44, no. 5: 892–898. <https://doi.org/10.2136/sssaj1980.03615995004400050002x>
- van Genuchten, M.Th., F.J. Leij, and S.R. Yates. 1991. The RETC code for quantifying the hydraulic functions. Version 1.0. U.S. Salinity Laboratory, USDA, ARS, Riverside, California.
- von Asmuth, J.R., K. Maas, M. Bakker, and J. Petersen. 2008. Modeling time series of ground water head fluctuations subjected to multiple stresses. *Groundwater* 46, no. 1: 30–40. <https://doi.org/10.1111/j.1745-6584.2007.00382.x>
- von Asmuth, J.R., M.F.P. Bierkens, and K. Maas. 2002. Transfer function-noise modeling in continuous time using predefined impulse response functions. *Water Resources Research* 38, no. 12: 23.1–23.12. <https://doi.org/10.1029/2001WR001136>
- Vonk, M.A., R.A. Collenteur, S. Panday, F. Schaars, and M. Bakker. 2024. Workflow and data of: Time series analysis of nonlinear head dynamics using synthetic data generated with a variably saturated model. <https://doi.org/10.5281/zenodo.8403295>.
- Wright, S. 1921. Correlation and causation. *Journal of Agricultural Research* 20, no. 7: 557–585.
- Zaadnoordijk, W.J., S.A.R. Bus, A. Lourens, and W.L. Berendrecht. 2019. Automated time series modeling for piezometers in the national database of The Netherlands. *Groundwater* 57, no. 6: 834–843. <https://doi.org/10.1111/gwat.12819>